arXiv:1512.03801v1 [cond-mat.supr-con] 11 Dec 2015

Charge orders, magnetism and pairings in the cuprate superconductors

T. Kloss[1], X. Montiel[1], V. S. de Carvalho[2], H. Freire[2], C. Pépin[1]
1. IPhT, L'Orme des Merisiers, CEA-Saclay, 91191 Gif-sur-Yvette, France and
2. Instituto de Física, Universidade Federal de Goiás, 74.001-970, Goiânia-GO, Brazil
(Dated: December 11, 2015)

We review the recent developments in the field of cuprate superconductors with the special focus on the recently observed charge order in the underdoped compounds. We introduce new theoretical developments following the study of the antiferromagnetic (AF) quantum critical point (QCP) in two dimensions, in which preemptive orders in the charge and superconducting (SC) sectors emerged, that are in turn related by an SU(2) symmetry. We consider the implications of this proliferation of orders in the underdoped region, and provide a study of the type of fluctuations which characterize the SU(2) symmetry. We identify an intermediate energy scale where the SU(2) pairing fluctuations are dominant and argue that they are unstable towards the formation of a Resonant Peierls Excitonic (RPE) state at the pseudogap (PG) temperature T^*. We discuss the implications of this scenario for a few key experiments.

I. INTRODUCTION

The last decade has seen a strong revival of interest in cuprate superconductors, with the observation of charge orders in the underdoped regime of these materials. Maybe the starting point of this intense period of investigation was the observation by STM of checkerboard-type patterns inside the vortices in Bi-2212 [1, 2]. Subsequent studies with Fermi surface reconstruction showed that this feature was generic [3, 4] (also verified in Bi-2201 [5, 6]) and that the charge patterns corresponded to two axial wave vectors $(0, Q_y)$ and $(Q_x, 0)$, incommensurate with the lattice periodicity, and the magnitude of the wave vectors decreases with oxygen-doping. The charge excitation was also found to be non-dispersive in temperature, and correlated with the "hot-spots" - the points of the Fermi surface where the AF zone boundary is intersected. The picture refined itself a bit later, and we now believe the charge order emerges at the tip of the Fermi arcs [7, 8]. The study of charge order in underdoped cuprates stayed in a *status quo* until the observation of quantum oscillations (QO) under a strong magnetic field in YBCO [9, 10]. This result pointed directly to a reconstruction of the Fermi surface induced by magnetic field and received several explanations in terms of stripe and charge patterns until the link was made with the bi-axial charge order observed by STM [11–14]. In particular, models for the reconstruction of the Fermi surface involved charge ordering with bi-axial wave vectors similar to those unveiled by STM. A subsequent Nuclear Magnetic Resonance (NMR) study finally found some charge splitting under a magnetic field $B \geq 17$T, which brought the final confirmation that charge order under a finite magnetic field is coherent, static and long-ranged [15–17]. The field versus temperature phase diagram was later completed by ultrasound experiments, which showed evidence for a flat transition line at $B_c = 17$T [18]. For $B \leq B_c$, YBCO is a d-wave superconductor. The increase of the magnetic field then creates vortices whose cores show the typical charge ordering [16]. For $B \geq B_c$ YBCO shows long range charge order with a typical ordering temperature remarkably similar in magnitude with the SC T_c. In the PG regime at $B = 0$, both hard x-ray [19, 20] and soft x-rays [21–24] study showed the presence of a sizable short range excitation at the bi-axial wave vectors. A softening of the phonon spectrum has been observed in the PG phase, while a softening at the charge order wave vectors occurs below T_c [25, 26]. Note that a recent state-of-the-art x-ray experiment at $B = 17$T showed that the charge order becomes uni-axial and tri-dimensional at high field [27]. One preliminary conclusion that one can infer from these experiments is that the charge and superconducting sectors are of the same order of magnitude in cuprate superconductors. We will use this observation later when we introduces the emergent SU(2) rotations that appear between these two sectors.

We turn now to one of the most enduring mysteries of cuprate superconductors, the pseudogap (PG) regime. The PG phase was observed in 1989 by NMR experiments [28, 29], where a gradual drop in the Knight-shift was observed at a crossover temperature T^*. This gap was attributed to a loss of density in the electronic carriers, and it was shown to decrease when the oxygen-doping increases but no obvious symmetry breaking was associated with this phase transition. We focus here on a few properties of the PG phase which we will use later in the SU(2)-interpretation of the experiments. The first remark that one can make is that the PG is an extremely robust feature of the phase diagram. It seems insensitive to disorder [30, 31] and magnetic field [32] and is closely associated to a regime of linear-in-T resistivity on its right hand side [33–35]. One other very striking observation in the PG regime detected by angle-resolved photoemission (ARPES), is the formation of Fermi arcs, instead of a closed-contour Fermi surface [36–41]. Recently, a momentum scale of similar magnitude as the one observed in the CDW was associated to the opening of the PG in the

anti-nodal region of the Brillouin zone (BZ) [42–44], and led to an interpretation in terms of a pair-density-wave (PDW) [45, 46]- or a finite momentum superconducting state Fulde-Ferrell-Larkin-Ovchinnikov (FFLO) [47, 48]. Coherent neutron scattering showed a $\mathbf{Q} = 0$ signal [49–54], which was interpreted in terms of intra-unit-cell loop currents [55–57]. Although a $\mathbf{Q} = 0$ phase is unable to open a gap in the electronic density of states, the loop-current line surprisingly follows the T^*-line. Note that NMR [58, 59] and μSR [60, 61] techniques were not able to detect such loop current. An explanation could be the longer time scale of local probes ($\approx 10^{-8} - 10^{-6}s$) compared with the INS time scale ($\approx 10^{-11}s$). At lower temperature, a Kerr effect signal has been reported, hinting at a breaking of time-reversal (TR) symmetry inside the PG [62]. This last observation is widely discussed by the community, but it is necessarily related to the $\mathbf{Q} = 0$ loop currents [63, 64]. The inelastic neutron scattering (INS) is also interesting for revealing collective modes of the system. A resonance at 41meV was found in YBCO the early days of cuprate superconductivity [65] and at similar energies in other compounds [66–69]. It was first believed that this collective excitation existed only in the SC phase, where it has a typical "hour-glass" shape centered around 41 meV at $\mathbf{Q} = (\pi, \pi)$, as a function of energy and wave-vector. It was later shown that the resonance exists as well in the PG phase above T_c, where it is still centered around 41 meV, but shows a typical "Y"-shape with a long energy-extension at $\mathbf{Q} = (\pi, \pi)$[70–73]. Many theoretical approaches have been invoked to describe the resonance below the SC transition [74–77]. This observation of the resonance around similar typical energies in the SC and PG phases, however, has never received a theoretical description, and constrains theories of the PG to keep some reminiscence of the SC phase. The neutron resonance was also observed in mono-layer tetragonal compounds (Hg-1201), where the long energy extension at $\mathbf{Q} = (\pi, \pi)$ persists below T_c [78].

Collective modes of a material give useful insights to probe symmetries of an effective model. One example is a resonance observed in the Raman A_{1g} channel, that appears at energies very similar to the ones where a collective mode was observed by INS [79–81]. Raman scattering typically probes the symmetries of the Fermi surface and the presence of "two gaps" in the underdoped regime of the cuprates was observed below T_c [82–84]. This fact was corroborated in a series of ARPES experiments on BSCO from which the gap velocity v_Δ at the nodes was extracted and shown to differ from the Fermi velocity. Three regions in the phase diagram were identified [85]. Starting from the over-doped region and decreasing the doping, v_Δ is shown to first increase then to reach a plateau in the underdoped region -down to dopings of the order of 5 %, and after that it drops at lower dopings when the system gets close to the insulating Mott-transition. The key question associated with the PG phase is whether it is a "strong-coupling" phenomenon, emerging as a direct consequence of the Mott transition [86–90], or whether it is a a very unusual collective phenomenon which is sensitive to other peculiarities of the physics of the cuprates, like its low dimensionality, the antiferromagnetic fluctuations or its fermiology [91–94]. In this work, we argue that the key to explain the mystery of the PG phase resides in an underlying emergent SU(2) symmetry, which produces SU(2) pairing fluctuations at intermediate energy scales. These fluctuations are in turn unstable toward the formation of a new kind of excitonic state, the (RPE) state, which is responsible for gapping out the Fermi surface in the anti-nodal region of the BZ [94].

The paper is organized as follows: In section II, we present the basics of the emergent symmetry model with SU(2) symmetry. Section III discusses the competition between the U(1) and SU(2) paring fluctuations in the framework of the non linear σ model. In particular, we propose to explain the PG state as a new type of charge order: the Resonant Peierls Excitonic (RPE) state coming from the SU(2) fluctuations. We also demonstrate that the CDW state is a secondary instability produced by U(1) fluctuations mediated by a Leggett mode. In section IV, we discuss the possible experimental evidence of this phase before to conclude in section V.

II. THE EMERGENT SU(2) SYMMETRY

The concept of emergent symmetry in the context of the cuprate superconductors can be traced back to the work of Yang and later Zhang [95, 96] where a representation with pseudo-spin operators was introduced which rotated the d-wave SC state onto a d-wave bi-partite charge order. The lowering and raising pseudo-spin operators η^+, $\eta^- = (\eta^+)^\dagger$, and η_z, which follow from the definition

$$\eta^+ = \sum_{\mathbf{k}} c^\dagger_{\mathbf{k}\uparrow} c^\dagger_{-\mathbf{k}+\mathbf{Q}\downarrow} \tag{1a}$$

$$\eta_z = \sum_{\mathbf{k}} \left(c^\dagger_{\mathbf{k}\uparrow} c_{\mathbf{k}\uparrow} + c^\dagger_{\mathbf{k}+\mathbf{Q}\downarrow} c_{\mathbf{k}+\mathbf{Q}\downarrow} - 1 \right). \tag{1b}$$

The operators (1) form an SU(2) Lie algebra. Noticeably, the η-pairing stat – which is equivalent to finite center of mass pairing of vector $\mathbf{Q} = (\pi, \pi)$, or FFLO state – is an eigenstate of the Hubbard Hamiltonian, both for positive and negative U. The simplest irreducible representation for the pseudo-spin is the triplet vector Δ_m, with $m =$

$\{-1,0,1\}$ defined as

$$\Delta_1 = -\frac{1}{\sqrt{2}}\sum_{\mathbf{k}} c^{\dagger}_{\mathbf{k}\uparrow}c^{\dagger}_{-\mathbf{k}\downarrow}, \tag{2a}$$

$$\Delta_0 = \frac{1}{2}\sum_{\mathbf{k},\sigma} c^{\dagger}_{\mathbf{k}\sigma}c_{\mathbf{k}+\mathbf{Q}\sigma}, \tag{2b}$$

$$\Delta_{-1} = -\Delta_1^{\dagger}, \tag{2c}$$

which represents the two conjugated s-wave SC states (Δ_{-1},Δ_1) and the charge ordering state Δ_0. The SU(2) pseudo-spin operators (1) rotate each component of the multiplet (2) into one another in the standard way (l is the rank of the irreducible representation Eq. (2), here $l=1$)

$$\left[\eta^{\pm},\Delta_m\right] = \sqrt{l\left(l+1\right)-m\left(m\pm 1\right)}\Delta_{m\pm 1}, \tag{3a}$$

$$\left[\eta_z,\Delta_m\right] = m\Delta_m. \tag{3b}$$

The effective theory describing the pseudo-spin symmetry is the $SO\left(4\right)$ $[SO\left(4\right)=\left(SU\left(2\right)\times SU\left(2\right)\right)/Z_2]$ non-linear σ-model which excites thermally from the SC state to the ordered state. This model describes transitions from one state to the other within the generic framework of "spin-flop" transitions. In the case above one has a pseudo spin-flop from the s-wave SC to the CDW states, whereas the standard spin-flop transition from easy axis to easy plane belongs to the SO(3) group [97]. The concept of SU(2)-symmetry was used later on in an effective theory of the PG leading to a rotation from the d-wave superconductor to the d-density wave state [98]. Here the generators of the symmetry are simply $i\eta^{+}$, $i\eta^{-}$ and η^{z} and the effective theory is the $O\left(4\right)$ non-linear σ-model. Let us mention a similar rotation between the nematic d-wave bond order $\Delta_{nem}=\frac{1}{2}\sum_{\mathbf{k}\sigma} d_{\mathbf{k}}c^{\dagger}_{\mathbf{k}\sigma}c_{\mathbf{k}\sigma}$ and d-wave states $\Delta^{+}_{dsc} = -\frac{1}{\sqrt{2}}\sum_{\mathbf{k}} d_{\mathbf{k}}c^{\dagger}_{\mathbf{k}\uparrow}c^{\dagger}_{\mathbf{k}\downarrow}$, and $\Delta^{-}_{dsc} = \frac{1}{\sqrt{2}}\sum_{\mathbf{k}} d_{\mathbf{k}}c_{\mathbf{k}\downarrow}c_{\mathbf{k}\uparrow}$ where $d_{\mathbf{k}}=\cos k_x-\cos k_y$ [99]. The pseudo-spin generators in this case take the form L^{+}, $L^{-}=\left(L^{+}\right)^{\dagger}$, L_0 with

$$L^{+} = \sum_{\mathbf{k}} c^{\dagger}_{\mathbf{k}\uparrow}c^{\dagger}_{-\mathbf{k}\downarrow}, \qquad L_0 = \sum_{\mathbf{k}\sigma}\left(c^{\dagger}_{\mathbf{k}\sigma}c_{\mathbf{k}\sigma}-1\right). \tag{4}$$

Note that the chemical potential couples to the generator η^{z} (or L_0) and thus a finite chemical potential breaks the SU(2) symmetry in favor of the SC state.

Another rotation, this time from the SC state towards the AF state, was introduced early on and became famous as the SO(5) theory [97, 101, 102] . The SO(5) theory is the one of a non-linear σ-model which operates on a five state "superspin" $\left(\ n_1,\ n_2,\ n_3,\ n_4,\ n_5\ \right)$-two SC states $\left(\ n_1=\Delta_s,\ n_5=\Delta_s^{\dagger}\ \right)$ and three AF vectors $\left(\ n_2=s^{+},\ n_3=s^{-},\ n_4=s^{z}\ \right)$ [97]. The superspin n_a is a vector representation of the SO(5) algebra. The SO(5) theory was based on the idea that both the SC and the AF states are key players of the physics of these compounds and are close enough in energy so that in between their respective phase transition an SO(5)-symmetric state is found where SC and AFM are undistinguishable. This phase was naturally associated with the PG of the cuprates. A typical SO(5) non-linear σ-model was introduced to describe the effective physics of the system, and four typical phase diagrams were derived which are depicted in Fig. 1. The mechanism favoring one of the states in the non-linear σ-model can be understood as a spin-flop transition- also called "super spin flop" transition for the SO(5) symmetries. As mentioned above, one gets a very accurate picture by thinking of the spin-flop transition of the antiferromagnetic state in a uniform magnetic field $\mathbf{B}$ along the easy$z$-axis [103, 104]. The magnetic field creates an easy plane xy, so that at a critical value of the field, the Néel wave vector changes its orientation abruptly from the z-axis to the xy-plane. Hence although in each of the above cases the symmetries are different, the underlying physics is as simple as the one on a spin-flop transition. The four typical phase diagrams show the various phases as a function of temperature and an external parameter which breaks the symmetry and are depicted in Fig. 1. They correspond to the cases where: 1) a first order transition between

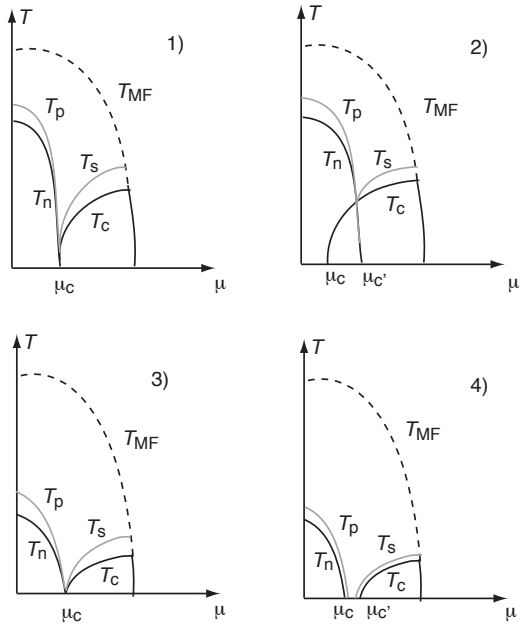

FIG. 1. (Color online) Schematic phase diagram of the SO(5) model [100]. Four types of scenarios are discussed in Ref. [100]: 1) a direct first order transition with a bi-critical point, 2) two second order transitions with an intermediate coexistence regime, 3) one single second order transition terminating at a QCP at zero temperature and 4) two second order transitions with a quantum disordered phase. Although the SO(5) symmetry is broken in scenario 1), 2) and 3) at zero temperature, thermal fluctuations lead to a restoration below the mean-field critical temperature T_{MF}. Adapted from Ref. [100].

the two states terminates at a bi-critical point; 2) there is a coexistence phase between the two orders; 3) the transition between the two orders terminates at $T = 0$ at a quantum critical point (QCP) or 4) the two orders are disconnected. In cases 1), 2) and 3), although the symmetry is broken at zero temperature, thermal fluctuations restore the SO(5)- or SU(2)- symmetry, leading to an invariant phase under the mean field transition T_{MF}. In the case of the SO(5)-symmetry, the typical phase diagram of the cuprates has the shape depicted in case 4), where the two orders are disconnected from one another, and this situation leads to a splitting of the big group to the $SO(3) \times U(1)$ subgroups describing fluctuations associated to each order separately. Furthermore, the SO(5) symmetry led to the prediction of a giant proximity effect in a SC-AF-SC junction [105, 106]. Unfortunately, this proximity effect was never verified experimentally [107]. One reason invoked here was that the SC state is by nature itinerant while the AF state is an insulator in those compounds. Hence the typical energy difference between those two states is big, of the order of the Coulomb U.

In the present work, we revive the concept of emergent symmetry, with an the SU(2) symmetry which rotates from a d-wave SC state to an incommensurate d-wave charge order. The pseudo-spin generators have the same form as depicted in Eqn. (1), with the exception that the wave vector $\mathbf{Q} = \mathbf{Q_0}$ is now the charge order wave vector and is not necessarily commensurate with the lattice. The $l = 1$ irreducible representation is given by the d-wave version of Eqn. (2) with namely $\Delta_0 = \chi_{CDW}$, $\Delta_1 = \Delta^\dagger_{dsc}$and $\Delta_{-1} = -\Delta^\dagger_1$, namely

$$\Delta_1 = -\frac{1}{\sqrt{2}} \sum_{\mathbf{k}} d_{\mathbf{k}} c^\dagger_{\mathbf{k}\uparrow} c^\dagger_{-\mathbf{k}\downarrow}, \tag{5a}$$

$$\Delta_0 = \frac{1}{2} \sum_{\mathbf{k},\sigma} d_{\mathbf{k}} c^\dagger_{\mathbf{k}\sigma} c_{\mathbf{k}+\mathbf{Q}\sigma}, \tag{5b}$$

$$\Delta_{-1} = \frac{1}{\sqrt{2}} \sum_{\mathbf{k}} d_{\mathbf{k}} c_{\mathbf{k}\downarrow} c_{-\mathbf{k}\uparrow}. \tag{5c}$$

The CDW ordering wave vector could be the axial CDW wave vector observed through many recent experiments (STM, Quantum oscillations, X-rays, ARPES) or it could be another wave vector carefully chosen so that the SU(2) symmetry is fully respected. As it turns out, the Eight Hot Spots (EHS) model depicted in Fig. 2 provides an exact realization of such a symmetry, as was first mentioned in Ref.[108–110]. This model is a simplified version of the spin-fermion model, which describes the vicinity of an AF QCP within a metallic substrate [111]. At this point it is useful to recall that the spin-fermion model played an important role at the beginning of the theoretical investigation on the cuprates [112–114]. For a recent link to strongly correlated systems note also Ref. [115]. Two different views were (and are still) competing for the understanding of the phase diagram of these compounds. Observing that the SC phase is close to a Mott insulator, a first group of theoreticians consider that the system is fundamentally strongly correlated, namely that the Coulomb energy $U = 1$eV is affecting the qualitative behavior down to very low temperatures [86, 90, 116]. This viewpoint has been extensively developed around the resonating valence bond (RVB) suggestion made by Anderson as early as 1987 [86], and now explored via extensive numerical calculations which can capture the strongly interacting behavior [90, 117]. Another part of the physics community defends the viewpoint that the Mott transition has a strong qualitative influence up to 6-7% doping, beyond which the physics of the system is mainly driven by the presence of AF fluctuations [118]. Proponents of this viewpoint hence start the theoretical investigation with the spin-fermion (SF) model which couples conduction electrons to AF paramagnon modes $\Phi = (\Phi^x, \Phi^y, \Phi^z)$ on the brink of criticality with the propagator

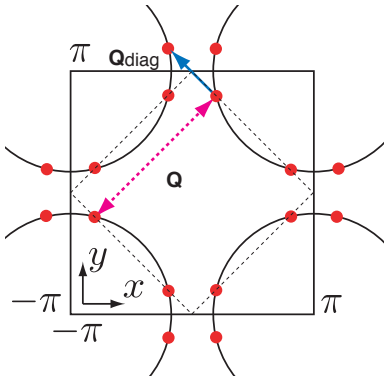

FIG. 2. (Color online) Schematic representation of the first Brillouin zone with the Fermi surface of cuprate superconductors. Hotspots are located at the intersection points of the AFM zone boundary with the Fermi surface. The diagonal coupling vector $\mathbf{Q}_{diag}$ between two hotspots is shown in blue and the AFM ordering vector $\mathbf{Q}$ in magenta.

$$\left\langle \Phi^\alpha_{\omega,\mathbf{q}} \Phi^\beta_{-\omega,-\mathbf{q}} \right\rangle = \frac{\delta_{\alpha\beta}}{c^{-2}\omega^2 + (\mathbf{q}-\mathbf{Q})^2 + \xi^{-2}_{AF}}, \tag{6}$$

where $\mathbf{Q}$ is the AF wave vector and ξ^{-1}_{AF} is the effective mass of the paramagnons which defines the distance to the QCP. Note, however, that in the present theory the SF model can be considered as an effective theory for which the SU(2) symmetry is approximately verified -in the case of hot regions [119], or exactly verified in the case of the EHS model [108, 110]. Although the proximity to the AF QCP may not be verified in the cuprates, we believe that the concept of emergent $SU(2)$ symmetry is robust and will remain when dust settles down. The conduction electrons have the kinetic energy $H_K = \sum_{k,\sigma} c^\dagger_{k,\sigma} \epsilon_k c_{k,\sigma}$ and interact with the paramagnons through a simple spin-spin interaction term $H_{int} = J \sum_i \mathbf{\Phi}_i \cdot c^\dagger_i \sigma c_i$. In the EHS model, a further

simplification is implemented with the reduction of the Fermi surface to eight "hot spots" which are the points at $T = 0$ where the electrons scatter through the AF Φ-modes. When the electron dispersion $\epsilon_k \simeq v_{hs}k$ is linearized at the hot spots, the model possesses an exact $SU(2)$ symmetry defined by the operators of Eqn. (1) but with $Q = Q_{diag}$, being the diagonal wave vector depicted in Fig. 2. This model was further studied in Ref.[110] and an $SU(2)$ precursor of the AF state was found, where quadrupolar density wave (QDW) with diagonal wave vector, which is equivalent to a d-wave CDW with diagonal wave vector, is degenerate with the d-wave SC state. This new state can be understood as a kind of non-Abelian superconductor with order parameter $\hat{b}$ that, instead of having a U(1) phase, has an $SU(2)$ unitary matrix fluctuating between the charge and SC sector [110, 119]

$$\hat{b} = b \begin{pmatrix} \Delta_{CDW} & \Delta_{SC} \\ -\Delta^*_{SC} & \Delta^*_{CDW} \end{pmatrix}_{SU(2)} \tag{7}$$

subject to the constraint $|\Delta_{CDW}|^2 + |\Delta_{SC}|^2 = 1$. Within the framework of the EHS model, and the related $O(4)$ non linear σ-model, several experimental findings were successfully addressed [120–122]. The general picture follows closely the ideas expressed in the $SO(5)$ theory, which are valid for all theories of emergent symmetries. A small curvature term in the electron dispersion breaks the symmetry in favor of the SC state. Hence at $T = 0$ the system is a superconductor. Once the temperature is raised, thermal fluctuations then excite the system between the two pseudo-spin states, restoring the $SU(2)$ invariance below the PG dome. Conversely, an applied magnetic field breaks the $SU(2)$ symmetry in favor of the CDW state and beyond a certain critical field B_c, a "pseudo spin-flop" is observed where the ground state "flips" from the SC state to CDW order. This "pseudo spin-flop" was precisely observed in experiments performed under magnetic field, with a critical field $B_c \sim 17T$ [9, 13, 123]. In particular, the ultrasound experiment [18] shows that the typical **B** versus T phase diagram in Fig. 3 is very similar to Fig.1-2). Within the EHS model, this experiment was addressed in Ref. [121]. Note that a co-existence phase is present in this phase diagram, which accentuates the similarity with the phase diagram 2) in Fig. 1 of the $SO(5)$ theory. Notice as well that the CDW and SC temperatures are of the same order of magnitude, which was never the case for the AF and SC states. It is another indication that the $SU(2)$ symmetry is more likely verified in the underdoped cuprates than the $SO(5)$ symmetry.

Of course, a question can be raised at this point, which is that the exact realization of the $SU(2)$ symmetry within the EHS model gives a charge wave vector on the diagonal, while only axial charge order was experimentally observed [1, 2, 6, 20, 21, 24, 42, 43, 124]. It is

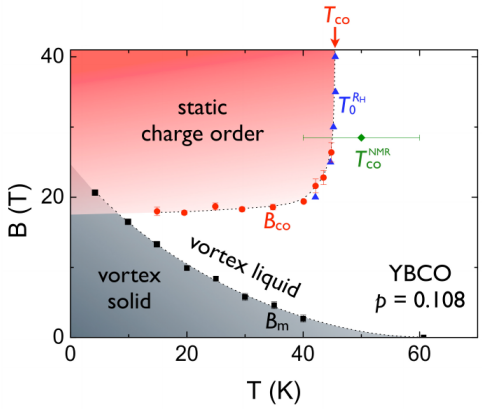

FIG. 3. (Color online) Experimental B-T phase diagram from sound velocity measurements in YBCO from Ref. [18]. The "pseudo spin-flop" is visible from the SC to CDW transition beyond a critical field $B_c \simeq 18$ T.

an important question in the $SU(2)$ theory and we will address it in details in the next section. For the moment let us notice that similar rotations as in Eqn.(1) can be generated for the axial wave vector $\mathbf{Q} = \{\mathbf{Q}_x, \mathbf{Q}_y\}$ observed experimentally, which rotates similar multiplets as in Eqn.(5) but for the axial wave vector. This idea of a rotation between the d-wave SC state and the axial charge order [122] was used to explain that the CDW signal is peaked at T_c [20, 21]. It was also used in explaining the A_{1g} mode observed in Raman scattering as a collective mode associated to this specific rotation [125–127].

The notion an emergent symmetry is more general than any of its specific representations. It is indeed very nice to have a model, although very simplified, where the $SU(2)$ symmetry is exactly realized (at all energy scales), but the main concern is whether this symmetry is approximately realized at finite temperatures in the underdoped region of the phase diagram. That is the interest of the concept of emergent symmetry: although it can be exactly realized in only a few effective models, if the splitting between the two pseudo-spin states is smaller than the typical energy of each state, it can also be approximately realized at low energies in the more realistic 2D $t-t'$ Hubbard model (this was verified explicitly in Refs. [128, 129] using two-loop RG techniques).

Another remark that can be made at this stage, is that another type of $SU(2)$ symmetry was identified early on, which consists of performing a particle-hole transformation on each site $c^\dagger_{i\sigma} \rightarrow c_{i-\sigma}$, which translates in the reciprocal space as $c^\dagger_{k\sigma} \rightarrow c_{k-\sigma}$ for all k vector. This symmetry is interesting for the phase diagram of the cuprates because it is exact at half-filling and will be gradually broken with doping [130, 131]. The operators for this

symmetry group take the form

$$\eta^{+}_{ph} = \sum_{\mathbf{k}} c^{\dagger}_{\mathbf{k}\uparrow} c^{\dagger}_{\mathbf{k}\downarrow} \tag{8a}$$

$$\eta_{z} = \sum_{\mathbf{k}\sigma} \left(c^{\dagger}_{\mathbf{k}\sigma} c_{\mathbf{k}\sigma} - 1 \right), \tag{8b}$$

while one irreducible $l = 1$ representation associated to it can be taken as [132]

$$\Delta_1 = -\frac{1}{\sqrt{2}} \sum_{\mathbf{k}} d_{\mathbf{k}} c^{\dagger}_{\mathbf{k}\uparrow} c^{\dagger}_{-\mathbf{k}\downarrow}, \tag{9a}$$

$$\Delta_0 = \frac{1}{2} \sum_{\mathbf{k},\sigma} d_{\mathbf{k}} c^{\dagger}_{\mathbf{k}\sigma} c_{-\mathbf{k}\sigma}, \tag{9b}$$

$$\Delta_{-1} = \frac{1}{\sqrt{2}} \sum_{\mathbf{k}} d_{\mathbf{k}} c_{\mathbf{k}\downarrow} c_{-\mathbf{k}\uparrow}. \tag{9c}$$

Interestingly, within the EHS model, the operators (8) and (9) are, respectively, the same as (1) and (5) with a diagonal wave vector, since there the summation over $\mathbf{k}$ is reduced to the eight hot spots. The EHS model is also an exact realization of the $SU(2)$ symmetry associated with particle-hole transformation.

Using (8) one can also ask oneself what is the $SU(2)$ partner of the observed axial CDW. To fix the ideas let us take a uni-axial CDW order with ordering wave vector $\mathbf{Q}_x$ relating two hot spots. One can then construct the $l = 1$ irreducible representation using the particle- hole transformation. This gives

$$\Delta_1 = -\frac{1}{\sqrt{2}} \sum_{\mathbf{k}} d_{\mathbf{k}} c^{\dagger}_{\mathbf{k}\uparrow} c^{\dagger}_{-\mathbf{k}+\mathbf{Q}_y\downarrow}, \tag{10a}$$

$$\Delta_0 = \frac{1}{2} \sum_{\mathbf{k},\sigma} d_{\mathbf{k}} c^{\dagger}_{\mathbf{k}\sigma} c_{\mathbf{k}+\mathbf{Q}_x\sigma}, \tag{10b}$$

$$\Delta_{-1} = \frac{1}{\sqrt{2}} \sum_{\mathbf{k}} d_{\mathbf{k}} c_{-\mathbf{k}+\mathbf{Q}_y\downarrow} c_{\mathbf{k}\uparrow}, \tag{10c}$$

which means that the $SU(2)$ partner of the $\mathbf{Q}_x$ CDW is the pair density wave (PDW), namely a non zero center of mass SC state, with $\mathbf{Q}_y$ wave vector. This notion of PDW state was introduced recently to explain the very unusual ARPES data tracing the formation of the PG in Bi-2201[45, 133]. In this theory, the formation of the PDW is suggested as the primary mechanism for the formation of the PG state, which means that the observed CDW is a secondary order. As such, it should be observed at a wave vector twice as big as the PDW wave vector $\mathbf{Q}_{CDW} = 2\mathbf{Q}_{PDW}$. In contrast, if the mechanism governing the underdoped region is a hidden pseudospin $SU(2)$ symmetry, then the partner of a bi-axial CDW is a bi-axial PDW with the same wave vectors $\mathbf{Q}_{CDW} = \mathbf{Q}_{PDW}$ (see the Refs. [46, 129, 134, 135]). The latter scenario has recently been verified experimentally [136].

III. NON LINEAR σ-MODEL, AND $SU(2)$ VS. $U(1)$ PAIRING FLUCTUATIONS

The idea of emergent symmetries received a recent critique, that when the group of symmetry is large enough, the symmetric phase is unstable to smaller subgroups [137]. For example, the symmetric phase associated to the $SO(5)$ symmetry which was intended to describe the PG shall decompose into the $SU(2) \times U(1)$ group describing fluctuations around the AF and SC phases respectively. Similarly, the $SU(2)$ symmetry which rotates between the CDW and SC channel shall decompose into the $U(1) \times U(1)$ groups. In this section, we consider seriously the criticism that the symmetric phase of large non-abelian groups is unstable, but wonder more particularly about the fate of SC fluctuations.

The role of SC fluctuations in the physics of cuprates is indeed very mysterious. We know that they are a few orders of magnitude more intense that in standard metals like Al, or Cu [138], but experiments detecting pure the Josephson effect were observed only a few tens of degrees above T_c [30, 139, 140]. In the deeply underdoped phase, $U(1)$ SC fluctuations form a dome shape that we will discuss further in this section [140–144] . Direct observation of pre-formed pairs in the PG phase was always negative, but a giant proximity effect was observed in the Lanthanum-compounds induced in the PG phase when it is surrounded by optimal SC phases [145–147]. The very easy injection of pairs from optimally doped into the PG phase suggests that the PG phase is related to the SC phase through a hidden symmetry. Such proximity effects were predicted in the case of the $SO(5)$ symmetry and never observed [105], but specific predictions in the case of the $SU(2)$ symmetry were never discussed in detail.

A. The $SU(2)$ SC fluctuations

In this section we assume that at an intermediate energy scale SC fluctuations are present, protected by an $SU(2)$ symmetry between the CDW and SC channel. The microscopic derivation of the non linear σ-model describing the $SU(2)$ fluctuations can be found, in the context of the EHS model in Ref.[110], and in the context where regions of the Brillouin zone instead of points are "hot" -or hot anti-nodal regions-, in Ref. [94]. The massless $O(4)$ effective free energy has the following form

$$F_{SU(2)} = \frac{T^2}{2} \sum_{\varepsilon,\omega} \int_{\mathbf{k},\mathbf{q}} tr \delta \hat{u}^{\dagger}_{-k,q} \left[J_{0,k} \omega^2 + J_{1,k} q^2 \right] \delta \hat{u}_{k,q} \tag{11}$$

where $\hat{u}_{\mathbf{k},\mathbf{q}} = \begin{pmatrix} \Delta_{CDW} & \Delta_{SC} \\ -\Delta^{*}_{SC} & \Delta^{*}_{CDW} \end{pmatrix}$ is the $SU(2)$ matrix associated with the condition $|\Delta_{CDW}|^2 + |\Delta_{SC}|^2 = 1$,

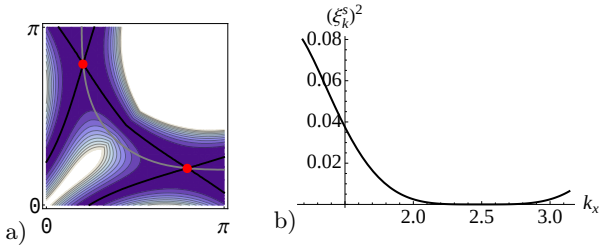

FIG. 4. (Color online) a) Visualization of the SU(2) symmetry breaking contribution $(\xi^s_{\mathbf{k}})^2$ in the positive region of the first Brillouin zone. It is small in the blue region and vanishes for the two black lines crossing the hotspot, but grows in the nodal line to the upper edge. b) Variation of $(\xi^s_{\mathbf{k}})^2$ along the Fermi surface (shown as a gray line in panel a)) parametrized as a function of k_x. While $(\xi^s_{\mathbf{k}})^2$ vanishes at the hotspot and stays small at the antinodes at $k_x = \pi$, it grows at the left side when approaching the nodal position.

and the tr runs on the $SU(2)$ structure. The coefficients write $J_{0,k} = |M_{\mathbf{k}}|^2 / |G^{-1}|^2$, and $J_{1,k} = J_{0,k} v^2_{\mathbf{k}}$, where $M_{\mathbf{k}}$ is the magnitude of the mean-field $SU(2)$ order parameter $\hat{M}_{\mathbf{k},\mathbf{q}} = \begin{pmatrix} & \hat{m}_{\mathbf{k},q} \\ \hat{m}^\dagger_{\mathbf{k},q} & \end{pmatrix}_\Lambda$, with $\hat{m}_{\mathbf{k},\mathbf{q}} = M_{\mathbf{k}} \hat{u}_{\mathbf{k},\mathbf{q}}$, which has a 4×4 structure in the $\tau \times \Lambda$-$SU(2)$ spaces where τ is the particle-hole transformation and Λ is the $\mathbf{Q}$-translation. The Green's function writes $\hat{G}^{-1} = \hat{G}^{-1}_{0,k} + \hat{M}_{k,0}$, with $\hat{G}^{-1}_{0,k} = i\omega - (\tau_3 \xi^s_{\mathbf{k}} - \xi^a_{\mathbf{k}})\,\Lambda_3$, with $\xi^{s,a}_{\mathbf{k}} = (\epsilon_{\mathbf{k}} \pm \epsilon_{-\mathbf{k}-\mathbf{Q}})/2$, and $\epsilon_{\mathbf{k}}$ being the electron dispersion. Note that no information was given on the value of the $\mathbf{Q}$-wave vector for the CDW sector. It corresponds in all generality to the $SU(2)$ operators (1) and (2). The exact $SU(2)$ symmetry is verified when $\xi^s_{\mathbf{k}} = 0$ which effectively kills the τ_3-term in the equation for $\hat{G}^{-1}_{0,k}$. $\xi^s_{\mathbf{k}}$ hence models the symmetry breaking term associated with this specific wave vector and contributing to the free energy as

$$F_{SB} = \frac{T^2}{2} \sum_{\varepsilon,\omega} \int_{\mathbf{k},\mathbf{q}} J_{3,k}\, tr\left[\delta\hat{u}^\dagger_{-k,q} \tau_3 \delta\hat{u}_{k,q} \tau_3\right], \qquad (12)$$

with

$$J_{3,k} = \frac{1}{4} \frac{|m_{0,k}|^2 (\xi^s_{\mathbf{k}})^2}{|G^{-1}|^2}. \qquad (13)$$

The shape of the symmetry-breaking term Eqn.(13) is visualized in Fig. 4. One can observe the anisotropy of the mass in various directions in the Brillouin Zone : the mass is much bigger in the nodal direction than in the anti-nodal one.

B. Resonant Peierls Excitonic (RPE) state

We now integrate the $SU(2)$ SC fluctuations out of the partition function, and evaluate the consequences of them in the charge channel. We get the following effective action

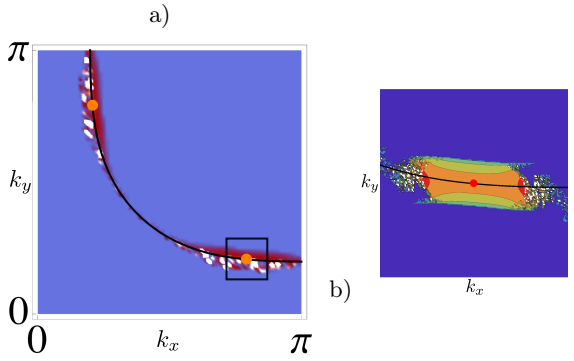

FIG. 5. (Color online) left) Density of the charge order parameter $|\chi_{k,-k}|$ in the first Brillouin zone from the RPE state. The charge density follows the Fermi surface, but due to a SU(2) dependent mass contribution, does not stabilize in the nodal region. right) Charge order parameter around the hotspot position for a constant $2\mathbf{p}_F$ ordering vector. From Ref. [94].

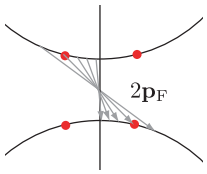

FIG. 6. (Color online) Set of degenerate $2\mathbf{p}_F$ couplings between electrons on opposed Fermi surfaces in the antinodal region due to the RPE state. From Ref. [94].

$$S_{\text{eff}}[c] = \sum_{\mathbf{k}\mathbf{k}'\mathbf{q}} \pi_{k,k',q} c^\dagger_{\uparrow\mathbf{k}} c_{\uparrow\mathbf{k}'} c^\dagger_{\downarrow-\mathbf{k}+q} c_{\downarrow-\mathbf{k}'+\mathbf{q}}, \qquad (14)$$

with

$$\pi_{k,k',q} = \langle \bar{\Delta}_{k,q} \Delta_{k',q} \rangle = \frac{\pi_0 \left(\delta_{k,-k'} + \delta_{k,k'}\right)}{(J_0 \omega_n^2 + J_1 (\mathbf{v}\cdot\mathbf{q})^2 + a_{0,k})}, \qquad (15)$$

where the form of the SC fluctuations comes from Eqns.(11,12). The self-consistent Dyson equation (or "gap equation") writes

$$\chi_{k,k'} = \sum_q \pi_{k,k',q} [\hat{G}(q-k, q-k')]_{12}, \qquad (16)$$

with $\chi_{k,k'} = \sum_q \pi_{k,k',q} \langle c^\dagger_{\sigma\mathbf{k}} c_{\sigma\mathbf{k}'} \rangle$ and with

$$\begin{aligned} [\hat{G}_{k,k'}]_{12} &= -\langle c^\dagger_\sigma(k) c_\sigma(k') \rangle \\ &= -\frac{\chi_{k,k'}}{(i\epsilon_n - \xi_{\mathbf{k}})(i\epsilon'_n - \xi_{k'}) - \chi^2_{k,k'}}. \end{aligned} \qquad (17)$$

To get some idea about the nonlocal nature the order parameter $\chi_{\mathbf{k},\mathbf{k}'}$, it is illustrative to consider one of the

labels having a constant shift $\mathbf{k}' = \mathbf{k} + \mathbf{P}$. The order parameter can then be decomposed as $\chi_{\mathbf{P},\mathbf{k}} = \chi_{\mathbf{P}} F_{\mathbf{P}}$ [94], where $\chi_{\mathbf{P}}$ is a plain wave and $F_{\mathbf{k}}$ a formfactor for the electron-hole pair with a finite extent, see Fig. 5b). The total order $\chi_{\mathbf{k},\mathbf{k}'}$ is thus a superposition of all local $\chi_{\mathbf{P},\mathbf{k}}$ orders, where $\mathbf{P}$ is running over the whole set of degenerate $2\mathbf{p}_{\mathrm{F}}$ couplings as visualized in Fig. 6. The gap in the antinodal region is $\Delta_{\mathbf{k}}^{PG} = \sum_{\{\mathbf{P}\}} \chi_{\mathbf{P},\mathbf{k}}$. Note that in Eqns. (16,17) the external wave vectors $\mathbf{k}, \mathbf{k}'$ are *a priori* not defined, but are let free to find self-consistently the most favorable solution. We studied numerically the possible excitonic solutions of the gap equations and the result is depicted in Fig. 5. We obtained an excitonic state in which a large number of wave vectors are degenerate with a typically $\mathbf{k} - \mathbf{k}' = 2\mathbf{k}_F$ which are spread out in the anti-nodal region of the Brillouin zone producing a depletion of the density of states in this region (see Fig. 6). Due to the angular dependence of the fluctuation mass ($a_{0,node} \gg a_{0,anti-node}$), we obtain a preferential gapping out of the anti-nodal region, which is characteristic of the $SU(2)$ SC fluctuations compared to the original $U(1)$.

C. Long range charge order

At this stage we have proposed a theory for the PG phase of cuprates superconductors. In the following we will give some more arguments that this theory is a promising candidate to describe high T_c superconductors. We know from a body of experimental evidence, though, that the PG phase is distinct from the observed uni-axial CDW. At zero field, the CDW dome decreases when the oxygen doping decreases, which is at variance with the PG T^*-line, which increases with the chemical potential (or oxygen doping) [21, 24, 124, 148–150]. Moreover, recent studies of the Fermi surface reconstruction under a magnetic field of 17 T infer that the PG is formed *before* the Fermi surface is reconstructed by CDW order -recall that the CDW becomes long range and three dimensional beyond $B = 17\,\mathrm{T}$. There are many proposals for the PG phase [45, 46, 90–92, 117, 122, 137, 151–154], but since ours consists of a special type of excitonic liquid, it is important to shed light on the relationship between the excitonic RPE phase and the observed axial CDW which is stabilized under magnetic field.

Within the EHS model, or within all sorts of simple weak coupling RPA evaluation, we find that the axial charge order is a secondary instability, weaker than CDW with a wave vector on the diagonal. The question that is then raised, is why nothing at all is observed on the diagonal, whether it is by STM [2, 5, 6, 8] or by X-rays [20, 21, 24, 148] The simplest explanation is that the pseudogap is forming, gapping out the anti-nodal region of the Brillouin Zone, and wiping out the CDW instability on the diagonal. When the mechanism of formation of the pseudogap instability has operated, then the secondary instability can be visible, at the tip of the Fermi arcs. Many suggestions have been made for the formation of axial CDW order. The fact that this wave vector is present as a secondary instability in any weak coupling theory, and stabilized for example, in the presence of additional effect like Coulomb interactions [134, 155, 156], within both one-loop and two-loop RG [128, 129, 157–159] or starting from a three band model [152], or invoking the proximity to the van Hove singularity [160] has been outlined in many works, including ours. All these studies are based on the observation that axial CDW is distinct from the formation of the PG state and starts to get formed at the tip of the arcs. In all mentioned scenarios though, it is quit unclear why the CDW dome is increasing with doping, in contrast with the PG line T^*. The $SU(2)$-paradigm which related the axial CDW to SC fluctuations that gives a good explanation for the maximum of amplitude of the CDW order at T_c [122] seems to have been lost in the attempts to rotate the leading wave vector from the diagonal to the axes.

In this paper, we would like to offer an alternative scenario which to our knowledge has not been proposed yet. It is based on the observation that the CDW dome follows closely the $U(1)$ SC fluctuation dome that can be detected through many probes, like resistivity study [30, 31], Nernst effect [141, 143, 144], Josephson tunneling. The $U(1)$ standard SC fluctuations are usually very weak in SC states because Coulomb interactions push them above the plasma frequency[161]. In the case of the optimally doped cuprates, due to low dimensionality, phase fluctuations are observed in a window of roughly 15 K above T_c [139]. For more underdoped compounds, the approach of the Mott insulating states produces a drastic increase of phase fluctuations due to the phase-particle number Heisenberg uncertainty relations [162]. We would like to exploit this idea here and suggest that the axial CDW order is an effect of the $U(1)$ SC fluctuations. We use a recent remark of Ref. [163] where it is noted that after the formation of the PG, the Fermi surface has split into four sections-or arcs, which are now independent from each other. In these conditions, one can get a Leggett mode between the tips of the arcs, which in turn can induce a charge order with the correct wave vectors, see Fig. 7. The gap equation for the axial CDW mediated by the Leggett mode writes

$$\chi_{\mathbf{k}\sigma,\mathbf{k}+\mathbf{Q_0}\sigma} = T \sum_{\omega_n \mathbf{q}} \pi_{\mathbf{Q_0},\mathbf{q}} [G_{-\mathbf{k}+\mathbf{q},-\mathbf{k}-\mathbf{Q_0}+\mathbf{q}}]_{12}, \qquad (18)$$

with $\mathbf{Q_0} = \mathbf{Q_{x/y}}$ being the axial wave vector, G_{12} given by Eqn.(17) with the replacement $\xi_{\mathbf{k}} \to \xi_{\mathbf{k}} + \Delta_{\mathbf{k}}^{PG}$ to take the gapping of the FS into account, whereas $\pi_{\mathbf{Q_0},\mathbf{q}}$ is the $U(1)$ correlation of the phase fluctuations at the tip of

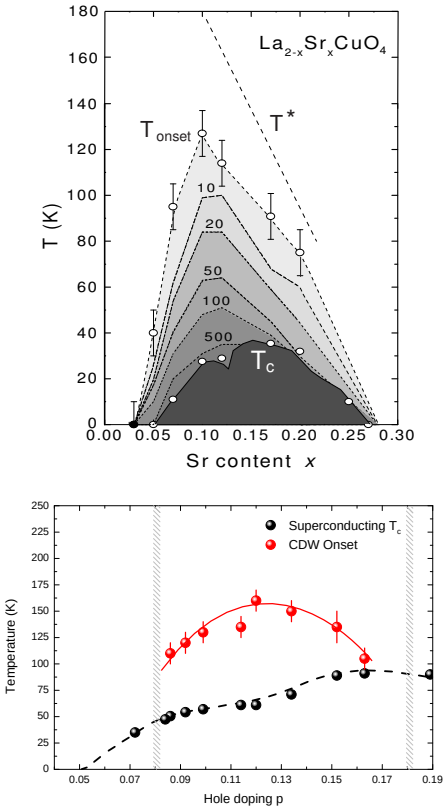

FIG. 7. (Color online) upper panel) Temperature-hole doping phase diagram deduced from Nernst effect experiments (from Ref.[144]). The gray area corresponds to CDW phase where Nernst coefficient is not zero. lower panel) Temperature-hole doping phase diagram with the superconducting critical temperature (black dots) and the onset temperature of the CDW axial order (red dots) deduced from RXS experiments in $YBa_2Cu_3O_{6+x}$ (extrated from Ref. [24]).

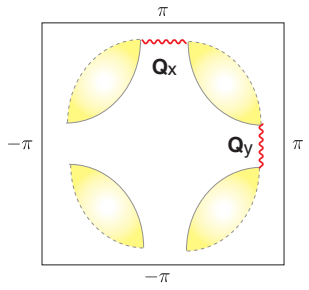

FIG. 8. (Color online) Leggett mode (highlighted in red), where charge order is induced by $U(1)$ phase fluctuations at the tip of the arcs with the axial wave vector $\mathbf{Q}_{x/y}$.

the arcs, as represented in Fig. 8

$$\pi_{\mathbf{Q_0},\mathbf{q}} = \left\langle \mathcal{T}\Delta_{\mathbf{k},-\mathbf{k}+\mathbf{q}}\Delta^{\dagger}_{\mathbf{k}+\mathbf{Q_0},-\mathbf{k}-\mathbf{Q_0}+\mathbf{q}} \right\rangle_{U(1)} = \frac{\pi_0}{J_0'\omega_n^2 + J_1'(\mathbf{v}\cdot\mathbf{q})^2 + m_0}, \quad (19)$$

with $\mathbf{k}$ being the wave vector at the tip of the one Fermi arc and $\mathbf{k}+\mathbf{Q_0}$ being the wave vector at the tip of the adjacent Fermi arc. We use a generic form of the propagator $\pi_{\mathbf{Q_0},\mathbf{q}}$, where π_0, J_0', J_1' and m_0 are mon-universal parameters the dependence on $\mathbf{Q}_0$ is neglected. We have performed a numerical study of Eqn.(18) which confirms that $U(1)$ SC fluctuations mediated by a Leggett mode produce axial CDW with the desired wave vector. This proposal has the merit to consistently link both the formation of the PG and the observed axial CDW to SC fluctuations, the former being described by the $SU(2)$ non linear σ-model while the latter are the standard $U(1)$ phase fluctuations.

IV. DISCUSSION

In the phase diagram of high temperature cuprates a few key players can be identified [131, 164]. There is at half-filling the Mott insulating transition with typical energy of 1 eV associated to it. Antiferromagnetism is ubiquitous in the whole phase diagram, with an ordered phase of typically $T_{Neel} \approx 700\,K$ at half-filling, very close to the Mott transition, and strong, but short range AF fluctuations in the underdoped regime. In the proposal of this paper, the mysterious PG phase of high temperature cuprates is attributed to a new kind of excitonic state, the RPE, which can be understood as a new type of "liquid" of excitons, with a superposition of degenerate wave vectors. This state is a consequence of integrating out the SC fluctuation, protected by an emergent $SU(2)$ symmetry between the SC and charge channel. In the discussion of this proposal, the first thing to recall is that although antiferromagnetism is not directly responsible for the PG, it is nevertheless the underlying force driving the emergence of precursor orders. In the early version of this theory, the EHS model has been studied as a reference model where the $SU(2)$ symmetry is verified [110, 165]. In this model the eight hot spots are singled out of the Fermi surface, and long range AFM fluctuations stabilize the composite $SU(2)$- order parameter, composed by a diagonal quadrupolar density wave and SC. In more generic versions of this theory, the model is extended to "hot regions" of the Brillouin zone - the anti-nodal regions, where AF acts predominantly and the $SU(2)$ symmetry is most strongly verified [119]. Antiferromagnetism did not disappear from the phase diagram, but rather has a very special relation to the PG by defining the width of the "hot regions", thus limiting the domain of action of the RPE state, and also being the driving force both behind SC pairing and the $SU(2)$ symmetry.

The concept of emergent symmetry though, is more robust and general than even the idea of Quantum Criticality and it is under such a generic paradigm that we want to cast out the underdoped region of cuprate superconductivity. The main idea is that charge orders are the natural partner and competitors of SC pairing in the un-

derdoped region of the cuprates, and typical pseudo "spin flops" between the two orders are to be expected, and we believe already observed under magnetic field [18].

The experimental consequences of a phase diagram controlled by an $SU(2)$ emergent pseudospin symmetry are numerous, and it is very likely that our proposal for the RPE state may be confirmed or in-firmed within the next few years.

1. *Spectroscopic signatures*

One can first ask about the spectroscopic signature of such an excitonic state. What can be seen in STM or X-rays. Our claim here is that we can reproduce the very recent findings on Bi-2212 [7, 166], that the pure d-wave component of the axial CDW extends up to the PG temperature, see Fig. 9. In the RPE state, indeed, the excitons form not only around many degenerate wave vectors, but with a finite width around each wave vector. The real space picture is that the particle-hole pairing

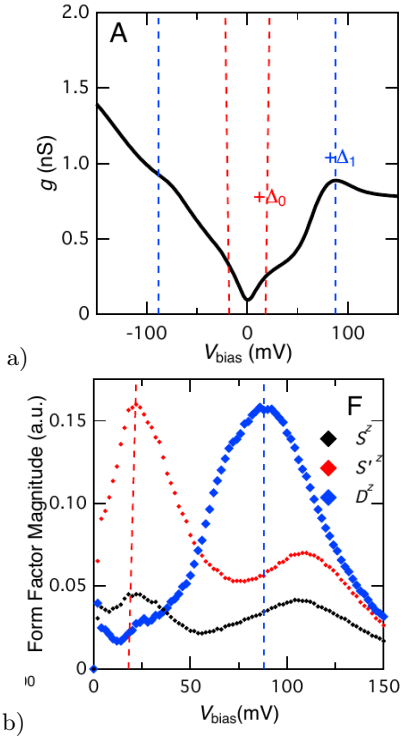

FIG. 9. (Color online) Upper panel a) Tunneling conductance measurements from Ref. [8] of underdoped cuprates. Two characteristic energies, a lower one for Bogoliubov quasiparticles and a higher one corresponding to the pseudogap are observed. Lower panel b) Energy dependence of the s- and d- wave form factors, indicating that the higher gap-energy scale corresponds to the d-wave form. From Ref. [8]

is non local in space, and modulated by many wave vectors. When the induced charge on the oxygen is evaluated and Fourier transformed, one finds that it is 90% d-wave (100 % for the diagonal wave vector and a bit less for the others), and at the same time, the axial wave vectors are more favored compared to the diagonal due to its nesting properties in the anti-nodal region [167]. The consequence is that the charge on the Oxygen shows a preponderant spectrum with axial wave vectors $\mathbf{Q}_x$ and $\mathbf{Q}_y$. At this stage our conclusion is that the RPE state is already observed by STM and X-rays, which have captured its preponderant contribution on the axial wave vectors.

2. *Proximity effect*

A second remark is that emergent symmetries rotating the SC phase to another type of order predict proximity effects when the PG phase is sandwiched between two optimally doped superconductors. The intensity of the induced current in the junction persists for thickness of the gap material much greater than the superconducting correlation length. This "Giant" Proximity Effect (GPE) is not explicable by the standard theory of the proximity effect between two SC junction, but can be understood in the situation where the SC state is "quasi-degenerate" to another phase of matter and Cooper pair can thus be easily injected from the SC state to the other state. The situation is thus very promising for emergent symmetries, and has been extensively studied in the case of the $SO(5)$-symmetry [102, 106], where specific predictions for the current as a function of the phase difference across the junction can be made as well for the $SU(2)$ symmetry, see Fig. 10. Note that a giant proximity effect has already been observed in various compounds but has not been observed for the specific setup of the $SO(5)$-group. One straightforward application of our theory is to check whether $SU(2)$ fluctuations, where the rotation is between the SC state and the CDW state can account for the experimental data [147, 168–173].

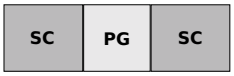

FIG. 10. (Color online) Proposition of a SC-PG-SC junction to study the giant proximity effect within the SU(2) theory. At a given temperature T that is homogeneous over the junction, the two outer SC layers are superconducing and at optimal doping such that $T < T_c$. The inner PG layer is an underdoped SC in the pseudogap phase ($T^* > T > T_c$). From the giant proximity effect we expect the PG phase to become superconducting by lowering the thickness of the inner layer.

3. Magnetic field phase diagram

The phase diagram found as a function of magnetic field and temperature, derived with a variety of experiments [9, 13, 16–18] is typical for a super "spin-flop" between two states related by a symmetry (see Fig.11). Note that three dimensional CDW has been recently observed by X-ray scattering above $B = 17$T [27]. The

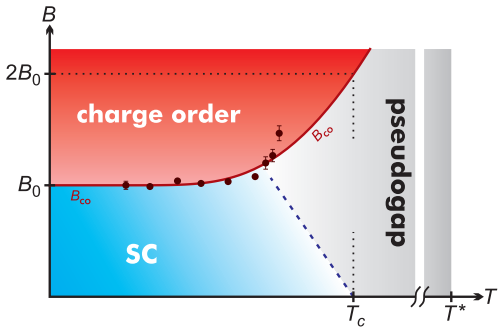

FIG. 11. (Color online) B-T phase diagram obtained from the spin-fermion model considering order parameter fluctuations around the mean-field value with a nonlinear σ model from Ref. [120].

CDW and SC orders have the same order of magnitude in this diagram, and the transition between the two is very sudden, like in a generic spin-flop XY model [120, 121]. Moreover, an $SU(2)$ partner of the axial CDW has recently been reported, i.e. the PDW with the same wave vector [136]. Although it is not a direct proof of the underlying symmetry, it seems to rule out other scenarios for the PG state where the PDW is primary while the CDW orders are secondary, and hence occur at twice the same wave vector as the PDW.

4. Collective modes

Emergent symmetries also have signatures in terms of collective modes. In a recent work we argued that the A_{1g}-mode observed in Raman scattering very close in energy to the neutron mode is such a signature of the SC-CDW $SU(2)$ symmetry [125], see Fig. 12. The collective mode used in this work was associated with the η-operator of Eqn.(1) with axial wave vector, thus associated to the triplet representation Eqn.(10). The presence of the two orders in conjunctions was needed in order for the Raman scattering vertex not to vanish. The model could account for the absence of observation of this order in the B_{1g} and B_{2g}channels.

Inelastic neutron scattering has reported since the very early days the presence of a collective mode in the underdoped regime, centered around the AFM wave vector $Q = (\pi, \pi)$, and at a finite energy around $E = 41$meV for the compound YBCO [65, 71]. Many theories, based

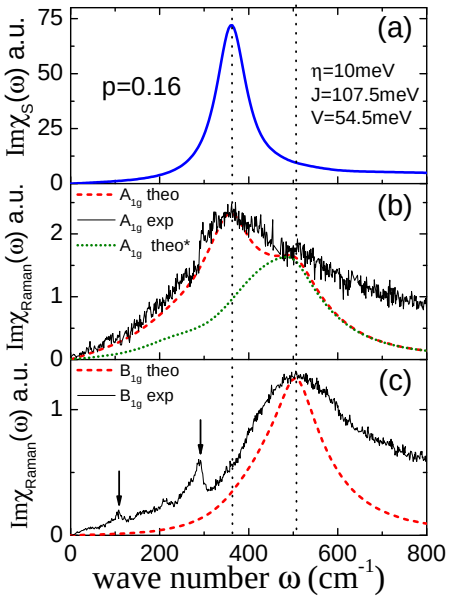

FIG. 12. (Color online) Raman scattering response from a collective mode. a) shows the calculated Neutron susceptibilities at the momentum $\mathbf{Q} = (\pi, \pi)$ as a function of the frequency. In b) (and c)), the experimental (solid line) and calculated (dashed line) Raman response in the A_{1g} (B_{1g}) Raman channels. The Raman resonance arises at the same frequency than the Neutron resonance at $\mathbf{Q}$ (Fig (a) and (b)) below the superconducting coherent peak energy observable in the B_{1g} symmetry (Fig (b) and (c)). This collective mode resonance appears in the A_{1g} symmetry since the Raman response is screened by long range Coulomb interaction in this symmetry. From Ref. [125].

on an RPA treatment of a magnetic spinon mode below the SC gap have been produced in order to explain this very characteristic feature of the cuprates [77, 102, 174]. The $SO(5)$ theory was originally devoted to the study of this mode [77]. The RPA theories, reproduce successfully the position of incommensurate signal around $Q = (\pi, \pi)$, having the typical "hour-glass" shape in the energy-momentum space. The present theories have difficulties to account for the fact that this signal remains inside the PG phase, changing form from the "hour-glass" to a "Y" shape, namely acquiring some extra low energy spectral weight at $Q = (\pi, \pi)$. The proposed RPE state is an excitonic state with excitations around a bunch of $2\mathbf{k}_F$- wave vectors in the anti-nodal region. Thus it behaves a little bit as a "charge superconductor", that in the simplest models, will gap out the electronic degrees of freedom precisely as a superconductor would do. We believe the RPE state can also account for the extra spectral weight at $Q = (\pi, \pi)$, which will be presented in a future work [167].

5. ARPES

We turn now to angle-resolved photoemission spectroscopy (ARPES), which have been very influential in our understanding of the PG phase of these materials, especially with the seminal observation of Fermi arcs in this phase . A recent ARPES experiment on Bi-2201 has been very important in our understanding of the formation of the PG [41, 43]. Dispersion cuts close to the Zone Edge show that the PG opens at a typical momentum larger than the momentum relating the two Fermi points $2\mathbf{k}_F$. Moreover when the dispersion cuts get closer to the nodes, the PG closes from below rather than from above. It has been argued that this set of peculiar features can only be explained by a PDW state (a finite momentum SC state), since only the particle-hole reversal specific to the pairing state can account for the closing of the gap from below [45, 175]. We argue that the RPE state

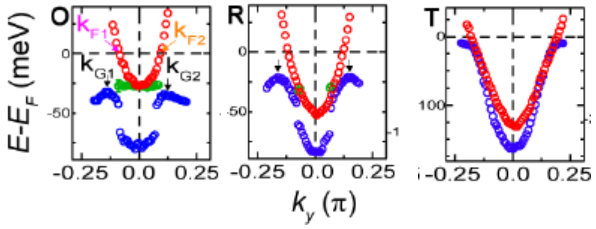

FIG. 13. (Color online) Electronic dispersion measured by ARPES in the superconducting (blue and green) and normal state (red). Cuts taken at constant k_x: close to the zone edge (O)($k_x = \pi$), close to the nodal region (T, $k_x = 0.6\pi$) and in an intermediate case (R, $k_x = 0.8\pi$). The closing of the gap can be observed from the antinodal to the nodal zone. From Ref. [43].

provides another explanation for this fascinating set of data. Besides the multiplicity of the wave vectors, the key ingredient is the non locality of the excitons. In particular, in the reciprocal space, they form within a finite window in the anti-nodal region, which can account for the natural closing in energy of the gap, both from above and below (ARPES does not see the positive energies), so that we have only to account for the negative part of the spectrum [167].

6. Loop currents

The observation of a $\mathbf{Q} = 0$ signal in neutron scattering at a temperature line following T^* [49] is one of the mysteries of the PG phase, which has been interpreted in terms of the formation of intra-unit-cell Θ_{II}-loop currents [90]. Although it is commonly understood that a $\mathbf{Q} = 0$ phase transition does not open a gap in the electronic spectrum, and thus the Θ_{II}-loop-current phase alone cannot be responsible for the origin of the PG, any proposal for the PG phase has to account for the signal observed in the neutron scattering experiment. We have

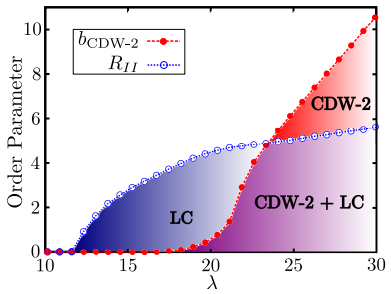

FIG. 14. (Color online) Coexistence between Θ_{II}-loop current order parameter and bidirectional d-wave CDW as a function of the interaction strength λ. From Ref. [135].

produced two studies within the EHS model regarding the possibility of coexistence of charge orders and loop currents [135, 159]. In Ref. [159], we have shown, within a saddle-point approximation, that the Θ_{II}-loop-current order cannot coexist with a d-wave CDW with diagonal wave vectors. As a result, we have offered this scenario as the possible reason, which explains why a d-wave charge order was never observed along the diagonal direction in the cuprates. In a subsequent work [135], we have demonstrated that a similar behavior is displayed by the d-wave CDW along axial directions described by uni-directional wave vectors (i.e. of the stripe-type), since the Θ_{II}-loop-current order is also detrimental to the latter order. By contrast, we have shown that bi-directional (i.e. checkerboard) d-wave CDW and PDW along axial momenta, which are in turn related by the emergent $SU(2)$ pseudospin symmetry pointed out previously, are compatible with the Θ_{II}-loop-current order, since all these orders can coexist with one another in the phase diagram (see, e.g., Fig. 14). These theoretical predictions agree, most spectacularly, with recent STM results [136] and also with x-ray experiments [24].

7. Pump probe experiment

A recent pump probe experiment also gives some evidence of the presence of strong SC fluctuations at an intermediate energy scale [176] in underdoped cuprates. In the first series of pump probe experiments [177, 178], the cuprate was excited up to 1.5 eV and relaxation at the pico-second scale - observed in the optical THz regime, destroyed the Cooper pairs and showed two typical energy scales, one related to the PG regime and one associated with the formation of the coherence SC phase. Those two scales are typically the ones observed, for example, in the dI/dV response of STM microscope. But in a recent experiment, the excitation was much weaker, in the mid Infra red regime [176] which enabled to scan

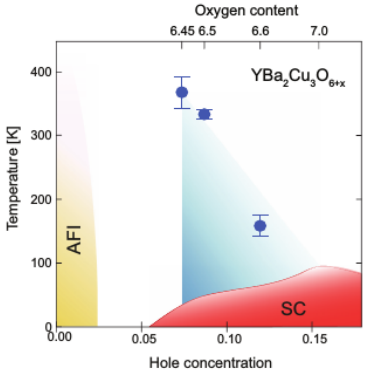

FIG. 15. (Color online) Schematic phase diagram for YBCO proposed in Ref. [176]. Under out-of-equilibrium conditions realized by optical pump-probes, a high mobility phase in the blue shaded area can be realized that extends much above the critical temperature of equilibrium SC. From Ref. [176].

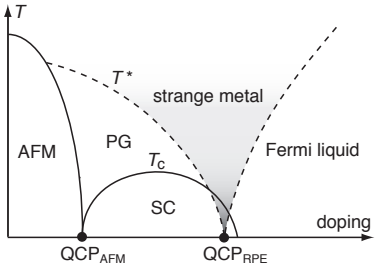

FIG. 16. (Color online) Schematic phase diagram of cuprate superconductors with the RPE state, as proposed in [94]. The quasi one-dimensional scattering in the vicinity of QCP_{RPE} produces the resistivity and the electronic self-energy anomaly observed in the strange metal phase. From Ref. [94].

the properties of the PG phase without destroying the Cooper pairs. What was found resembles to a pico-second photograph of SC fluctuations with the superfluid density $\rho_s \sim \omega\Delta\sigma_2$ shooting up in the PG phase, up to temperatures of 300 K , see Fig. 15. This pico-second "photograph" of the superfluid density was shown to follow the PG temperature as a function of doping.

8. *General phase diagram*

A general look at the phase diagram of the cuprates singles out many enduring mysteries, and one of the most enduring one is the linear-in-T resistivity around optimal doping. This phase was identified in a seminal work as a Marginal Fermi Liquid (MFL) [179, 180], and it is still a challenge for theories to account for this phenomenon. Recent in-depth experiments show a more complex behavior of the resistivity with temperature, with a part linear in T and a residual part going like T^2 when the strange metal regime is approached from the right hand side of the phase diagram [33, 34]. Two schools of ideas have been advanced to explain this very unusual phenomenon. In the first school of ideas, it is believed that the proximity to the Mott transition creates a very strongly correlated electronic medium where the electron mean free path is so weak that we are above the Ioffe-Regel limit for the MFL regime [87]. The second school of ideas advances that the resistivity slope as a function of temperature is very steep, so that the second MFL regime extends far beyond the Ioffe-Regel limit at low enough temperatures. Within this second viewpoint, the challenge is to suggest a QCP beyond the dome which could produce a very resistive scattering behavior for the conduction electrons. It is precisely what the quantum critical version of the RPE state does. Electronic scattering through quantum critical excitonic modes shows a quasi-one dimensional behavior, each electron scattering preferentially through its most favorable $2\mathbf{k}_F$ wave vector [94], and produces a resistivity that behaves as $\rho \sim T/\log T$ within a Boltzmann semiclassical calculation and the electronic self-energy that reads $\Sigma(i\epsilon_n) \sim i\epsilon_n/\log|\epsilon_n|$ in the "Strange Metal" (SM) regime (see Fig. 16). On the same line of thought, maybe one of the most difficult feature of the PG to account for in any theory is that it is insensitive to a large amount of Zn-doping or irradiation by electrons [31, 140, 181], which locate on Cu sites and produce strong disorder which exclude the doped Cu-site in the unitary limit [182]. The T^*-line is not affected and also the slope of the resistivity in the SM regime does not change [31]. It is difficult for any state of matter to have the sufficient robustness to show no sensitivity to such a strong perturbation. One way the RPE state could resist is through the non-locality of the excitons (i.e. the particles-hole pair), which can typically being created at site $\mathbf{r}$ and removed at site $\mathbf{r}'$ with the typical correlation $\langle c^\dagger_{\mathbf{r}} c_{\mathbf{r}'} \rangle$ [167].

V. CONCLUSION

To conclude, within the two large views of the cuprates where, on one hand, the physics of the PG is solely determined by strong correlations and the proximity to the Mott transition, and the other view where the qualitative features of the physics of the PG are governed by some hidden symmetry, the present work makes a clear discrimination in favor of the latter. It is claimed here that the physics of the PG and the SM phase are controlled by an emergent $SU(2)$ symmetry. Many properties of the underdoped cuprates can be captured within the pseudo-spin theory, the non-linear σ-model associated to this symmetry and the pseudo spin-flop physics between the SC and charge channel. We also claim that $SU(2)$ superconducting fluctuations proliferate at intermediate energy scales in the physics of these compounds, and are are the key ingredient to understand the PG

phase. At lower energy, they lead to the formation of the RPE state, which we believe has a lot of promising features to be the solution for the PG. At even lower temperatures, the $U(1)$ phase fluctuations enter the game and produce coherent axial CDW mediated by a Leggett-mode. The $SU(2)$ symmetry is present in the background of the whole underdoped region, and it is expected that pseudo-spin partners of the various orders (such as the PDW partner of the CDW order) have recently been observed experimentally [136]. Lastly, what is the influence of the Mott transition on the phase diagram of the cuprates ? We believe it will qualitatively affect the physics up to roughly 6% of doping. Below 6% of doping, techniques adequate to describe the very strongly coupled regime will capture the physics [82, 90, 117] . Beyond 6% doping, the physics is qualitatively protected by the $SU(2)$ symmetry. A very revealing experiment is the variation of the nodal velocity v_Δ as a function of doping extracted from ARPES data (Ref. [85]). A tri-sected dome is observed with three distinct regimes, 1) below 6% doping, 2) between 6% and 19% of doping and 3) above 19 % of doping. Within the $SU(2)$ theory, as with all theories controlled by an emergent symmetry, the critical value of 6% of doping is precisely the point where the Mott physics becomes dominant. Within the strongly correlated viewpoint, the typical doping of 6% is difficult to interpret.

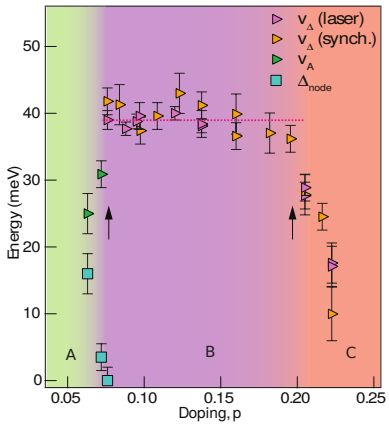

FIG. 17. (Color online) ARPES experiments on BSCO performed in Ref. [85]. The doping dependence of the gap velocity v_Δ reveals three distinct regime: two regions at low and high doping where v_Δ drops and a third regime in-between, where v_Δ reaches a plateau. From Ref. [85].

We are grateful to H. Alloul, Y. Sidis, P. Bourges and A. Ferraz for stimulating and helpful discussions. This work was supported by LabEx PALM (ANR-10-LABX-0039- PALM), ANR project UNESCOS ANR-14-CE05-0007, as well as the grant Ph743-12 of the COFECUB. CP and TK also acknowledge hospitality at the IIP (Natal, Brazil) where parts of this work were done.

[1] J. E. Hoffman et al., Science **295**, 466 (2002).
[2] K. Fujita et al., Science **344**, 612 (2014).
[3] M. Vershinin, Science **303**, 1995 (2004).
[4] E. H. da Silva Neto et al., Science **343**, 393 (2014).
[5] Y. He et al., Science **344**, 608 (2014).
[6] W. D. Wise et al., Nat. Phys. **4**, 696 (2008).
[7] M. H. Hamidian et al., arXiv:1508.00620 [cond-mat.supr-con] (2015).
[8] Hamidian M. H. et al., Nat Phys (2015).
[9] N. Doiron-Leyraud et al., Nature **447**, 565 (2007).
[10] D. LeBoeuf et al., Nature **450**, 533 (2007).
[11] N. Doiron-Leyraud et al., Phys. Rev. X **3**, 021019 (2013).
[12] S. E. Sebastian et al., PNAS **107**, 6175 (2010).
[13] S. E. Sebastian et al., Phys. Rev. Lett. **108**, 196403 (2012).
[14] O. Cyr-Choinière et al., arXiv: 1503.02033 [cond-mat.supr-con] (2015).
[15] T. Wu et al., Nature **477**, 191 (2011).
[16] T. Wu et al., Nat. Commun. **4**, 2113 (2013).
[17] T. Wu, H. Mayaffre, S. Krämer, and M. Horvatić, Nature **6**, 6438 (2015).
[18] D. LeBoeuf et al., Nat. Phys. **9**, 79 (2013).
[19] J. Chang et al., Nat Phys **8**, 871 (2012).
[20] E. Blackburn et al., Phys. Rev. Lett. **110**, 137004 (2013).
[21] G. Ghiringhelli et al., Science **337**, 821 (2012).
[22] M. Le Tacon et al., Nat. Phys. **7**, 725 (2011).
[23] S. Blanco-Canosa et al., Phys. Rev. Lett. **110**, 187001 (2013).
[24] S. Blanco-Canosa et al., Phys. Rev. B **90**, 054513 (2014).
[25] E. Blackburn et al., Phys. Rev. B **88**, 054506 (2013).
[26] M. Le Tacon et al., Nat. Phys. **10**, 52 (2014).
[27] J. Chang et al., arXiv:1511.06092 [cond-mat.supr-con] (2015).
[28] H. Alloul, T. Ohno, and P. Mendels, Phys. Rev. Lett. **63**, 1700 (1989).
[29] W. W. Warren et al., Phys. Rev. Lett. **62**, 1193 (1989).
[30] H. Alloul, F. Rullier-Albenque, B. Vignolle, D. Colson, and A. Forget, EPL (Europhysics Letters) **91**, 37005 (2010).
[31] F. Rullier-Albenque et al., EPL (Europhysics Letters) **50**, 81 (2000).
[32] F. Rullier-Albenque et al., Physical Review Letters **99**, 027003 (2007).
[33] N. E. Hussey, J. Phys. Condens. Matter **20**, 123201 (2008).
[34] N. E. Hussey et al., Philosophical Transactions of the Royal Society A: Mathematical, Physical and Engineering Sciences **369**, 1626 (2011).
[35] R. A. Cooper et al., Science **323**, 603 (2009).
[36] J. C. Campuzano et al., Nature **392**, 157 (1998).
[37] J. C. Campuzano et al., Phys. Rev. Lett. **83**, 3709 (1999).
[38] U. Chatterjee et al., Phys. Rev. Lett. **96**, 107006 (2006).
[39] A. Kanigel et al., Phys. Rev. Lett. **99**, 157001 (2007).
[40] K. M. Shen et al., Phys. Rev. Lett. **93**, 267002 (2004).
[41] K. M. Shen et al., Science **307**, 901 (2005).
[42] K. M. Shen, Science **307**, 901 (2005).
[43] R.-H. He et al., Science **331**, 1579 (2011).

[44] T. Yoshida, M. Hashimoto, I. M Vishik, Z.-X. Shen, and A. Fujimori, Journal of the Physical Society of Japan **81**, 011006 (2012).
[45] P. A. Lee, Phys. Rev. X **4**, 031017 (2014).
[46] Y. Wang, D. F. Agterberg, and A. Chubukov, Phys. Rev. Lett. **114**, 197001 (2015).
[47] P. Fulde and R. A. Ferrell, Physical Review **135**, A550 (1964).
[48] A. I. Larkin and Y. N. Ovchinnikov, Sov. Phys. JETP **20**, 762 (1965).
[49] B. Fauqué et al., Phys. Rev. Lett. **96**, 197001 (2006).
[50] Y. Li et al., Nature **455**, 372 (2008).
[51] P. Bourges and Y. Sidis, Comptes Rendus Physique **12**, 461 (2011).
[52] Y. Sidis and P. Bourges, J. Phys.: Conf. Ser. **449**, 012012 (2013).
[53] L. Mangin-Thro et al., Phys. Rev. B **89**, 094523 (2014).
[54] L. Mangin-Thro, Y. Sidis, A. Wildes, and P. Bourges, Nature Communications **6**, 7705 (2015).
[55] C. M. Varma, Phys. Rev. B **73**, 155113 (2006).
[56] V. Aji and C. M. Varma, Phys. Rev. B **75**, 224511 (2007).
[57] V. Aji and C. M. Varma, Phys. Rev. Lett. **99**, 067003 (2007).
[58] S. Strässle, B. Graneli, M. Mali, J. Roos, and H. Keller, Phys. Rev. Lett. **106**, 097003 (2011).
[59] A. M. Mounce et al., Phys. Rev. Lett. **111**, 187003 (2013).
[60] G. J. MacDougall et al., Phys. Rev. Lett. **101**, 017001 (2008).
[61] J. E. Sonier et al., Phys. Rev. Lett. **103**, 167002 (2009).
[62] J. Xia et al., Phys. Rev. Lett. **100**, 127002 (2008).
[63] V. Aji, Y. He, and C. M. Varma, Physical Review B **87**, 174518 (2013).
[64] V. M. Yakovenko, Physica B-Condensed Matter **460**, 159 (2015).
[65] J. Rossat-Mignod et al., Physica C **185-189, Part 1**, 86 (1991).
[66] P. Bourges et al., Physica C **424**, 45 (2005).
[67] H. He et al., Phys. Rev. Lett. **86**, 1610 (2001).
[68] H. F. Fong et al., Nature **398**, 588 (1999).
[69] H. He et al., Science **295**, 1045 (2002).
[70] P. Bourges et al., Science **288**, 1234 (2000).
[71] V. Hinkov et al., Nature **430**, 650 (2004).
[72] V. Hinkov et al., Nat. Phys. **3**, 780 (2007).
[73] S. M. Hayden, H. A. Mook, P. Dai, T. G. Perring, and F. Dogan, Nature **429**, 531 (2004).
[74] M. R. Norman, Phys. Rev. B **75**, 184514 (2007).
[75] M. Eschrig and M. R. Norman, Physical Review Letters **85**, 3261 (2000).
[76] I. Eremin, D. Morr, A. Chubukov, K. Bennemann, and M. Norman, Physical Review Letters **94**, 147001 (2005).
[77] E. Demler and S.-C. Zhang, Phys. Rev. Lett. **75**, 4126 (1995).
[78] W. Tabis et al., Nat. Commun. **5**, 5875 (2014).
[79] Y. Gallais, A. Sacuto, and D. Colson, Physica C **408 - 410**, 785 (2004).
[80] S. Blanc et al., Physical Review B **80**, 140502 (2009).
[81] S. Benhabib et al., Phys. Rev. B **92**, 134502 (2015).
[82] M. Le Tacon et al., Nat. Phys. **2**, 537 (2006).
[83] M. Civelli, M. Capone, A. Georges, and K. Haule, Physical Review Letters (2008).
[84] S. Blanc et al., Physical Review B **82**, 144516 (2010).
[85] I. M. Vishik et al., PNAS **109**, 18332 (2012).
[86] P. W. Anderson, Science **235**, 1196 (1987).
[87] A. Georges, G. Kotliar, W. Krauth, and M. J. Rozenberg, Rev. Mod. Phys. **68**, 13 (1996).
[88] A. Katanin and A. Kampf, Phys. Rev. Lett. **93**, 106406 (2004).
[89] G. Sordi, P. Sémon, K. Haule, and A. M. S. Tremblay, Scientific Reports **2** (2012).
[90] E. Gull, O. Parcollet, and A. J. Millis, Phys. Rev. Lett. **110**, 216405 (2013).
[91] K. Le Hur and T. M. Rice, Annals of Physics **324**, 1452 (2009).
[92] T. M. Rice, K.-Y. Yang, and F. C. Zhang, Rep. Prog. Phys. **75**, 016502 (2012).
[93] D. Chowdhury and S. Sachdev, The Enigma of the Pseudogap Phase of the Cuprate Superconductors, in *50th Karpacz Winter School of Theoretical Physics*, pages 1–43, WORLD SCIENTIFIC, 2015.
[94] T. Kloss, X. Montiel, and C. Pépin, arXiv:1510.03038 [cond-mat.supr-con] (2015).
[95] C. N. Yang, Phys. Rev. Lett. **63**, 2144 (1989).
[96] C. N. Yang and S. C. Zhang, Modern Physics Letters B **04**, 759 (1990).
[97] S. C. Zhang, Science **275**, 1089 (1997).
[98] C. Nayak, Phys. Rev. B **62**, R6135 (2000).
[99] H.-Y. Kee, H. Doh, and T. Grzesiak, JOURNAL OF PHYSICS CONDENSED MATTER **20** (2008).
[100] S.-C. Zhang, Science **275**, 1089 (1997).
[101] S. C. Zhang, J. P. Hu, E. Arrigoni, W. Hanke, and A. Auerbach, Physical Review B **60**, 13070 (1999).
[102] E. Demler, W. Hanke, and S.-C. Zhang, Rev. Mod. Phys. **76**, 909 (2004).
[103] S. Chakravarty, B. Halperin, and D. Nelson, Physical Review Letters (1988).
[104] S. Chakravarty, B. I. Halperin, and D. R. Nelson, Physical Review B **39**, 2344 (1989).
[105] E. Demler, A. J. Berlinsky, C. Kallin, and G. B. Arnold, Physical Review Letters **80**, 2917 (1998).
[106] B. C. den Hertog, A. J. Berlinsky, and C. Kallin, Physical Review B **59**, R11645 (1999).
[107] I. Bozovic, G. Logvenov, M. Verhoeven, and P. Caputo, Nature **422**, 873 (2003).
[108] M. A. Metlitski and S. Sachdev, New J. Phys. **12**, 105007 (2010).
[109] M. A. Metlitski and S. Sachdev, Phys. Rev. B **82**, 075127 (2010).
[110] K. B. Efetov, H. Meier, and C. Pépin, Nat. Phys. **9**, 442 (2013).
[111] A. Abanov and A. V. Chubukov, Phys. Rev. Lett. **84**, 5608 (2000).
[112] V. Barzykin and D. Pines, Phys. Rev. B **52**, 13585 (1995).
[113] D. J. Scalapino, Numerical Studies of the 2D Hubbard Model, in *Handbook of High-Temperature Superconductivity*, pages 495–526, Springer New York, New York, NY, 2007.
[114] P. Monthoux, D. Pines, and G. G. Lonzarich, Nature **450**, 1177 (2007).
[115] A. Ferraz and E. Kochetov, Europhys. Lett. **109**, 37003 (2015).
[116] P. W. Anderson et al., J. Phys. Condens. Matter **16**, R755 (2004).
[117] G. Sordi, P. Sémon, K. Haule, and A.-M. S. Tremblay, Phys. Rev. Lett. **108**, 216401 (2012).

[118] A. Chubukov, D. Pines, and J. Schmalian, *J 2003 The Physics of Conventional and Unconventional Superconductors vol 1ed K.H. Bennemann and J. B. Ketterson*, Berlin:Springer, 2003.

[119] T. Kloss, X. Montiel, and C. Pépin, Phys. Rev. B **91**, 205124 (2015).

[120] H. Meier, M. Einenkel, C. Pépin, and K. B. Efetov, Phys. Rev. B **88**, 020506 (2013).

[121] M. Einenkel, H. Meier, C. Pépin, and K. B. Efetov, Phys. Rev. B **90**, 054511 (2014).

[122] L. E. Hayward, D. G. Hawthorn, R. G. Melko, and S. Sachdev, Science **343**, 1336 (2014).

[123] T. Wu et al., Phys. Rev. B **88**, 014511 (2013).

[124] A. J. Achkar et al., Phys. Rev. Lett. **113**, 107002 (2014).

[125] X. Montiel et al., arXiv:1504.03951 [cond-mat.supr-con] (2015).

[126] A. Sacuto et al., Rep. Prog. Phys. **76**, 022502 (2013).

[127] Y. Gallais et al., Phys. Rev. Lett. **88**, 177401 (2002).

[128] V. S. de Carvalho and H. Freire, Ann. Physics **348**, 32 (2014).

[129] H. Freire, V. S. de Carvalho, and C. Pépin, Physical Review B **92**, 045132 (2015).

[130] G. Kotliar and J. Liu, Phys. Rev. B **38**, 5142 (1988).

[131] P. A. Lee, N. Nagaosa, and X.-G. Wen, Rev. Mod. Phys. **78**, 17 (2006).

[132] Note that a different representation was used in the slave-boson approaches [130, 131], where the rotation was performed from the d-wave SC state towards π-flux phases.

[133] D. F. Agterberg, D. S. Melchert, and M. K. Kashyap, Phys. Rev. B **91**, 054502 (2015).

[134] C. Pépin, V. S. de Carvalho, T. Kloss, and X. Montiel, Phys. Rev. B **90**, 195207 (2014).

[135] V. S. de Carvalho, C. Pépin, and H. Freire, arXiv:1511.03279 [cond-mat.supr-con] (2015).

[136] M. H. Hamidian et al., arXiv:1511.08124 [cond-mat.supr-con] (2015).

[137] E. Fradkin, S. A. Kivelson, and J. M. Tranquada, Rev. Mod. Phys. **87**, 457 (2015).

[138] Emery, V. J. and S. A. Kivelson, Nature **374**, 434 (1995).

[139] N. Bergeal et al., Nature Physics **4**, 608 (2008).

[140] F. Rullier-Albenque, H. Alloul, and G. Rikken, Physical Review B **84**, 014522 (2011).

[141] L. Li, N. Alidoust, J. M. Tranquada, G. D. Gu, and N. P. Ong, Physical Review Letters **107**, 277001 (2011).

[142] L. Li, Y. Wang, and N. P. Ong, Physical Review B , 056502 (2013).

[143] Y. Wang et al., Physical Review Letters **88**, 257003 (2002).

[144] Y. Wang, L. Li, and N. P. Ong, Physical Review B **73**, 024510 (2006).

[145] R. S. Decca, H. D. Drew, E. Osquiguil, B. Maiorov, and J. Guimpel, Phys.Rev.Lett. **85**, 3708 (2000).

[146] I. Bozovic et al., Phys.Rev.Lett. **93**, 157002 (2004).

[147] M. Elvezio et al., Nat Commun **2**, 272 (2011).

[148] A. J. Achkar et al., Phys. Rev. Lett. **109**, 167001 (2012).

[149] M. Bakr et al., Phys. Rev. B **88**, 214517 (2013).

[150] O. Cyr-Choiniere et al., arXiv:1504.06972 [cond-mat.supr-con] (2015).

[151] T. Senthil, S. Sachdev, and M. Vojta, Phys. Rev. Lett. **90**, 216403 (2003).

[152] S. Bulut, A. P. Kampf, and W. A. Atkinson, arXiv:1503.08896 [cond-mat.supr-con] (2015).

[153] L. Nie, L. E. Hayward Sierens, R. G. Melko, S. Sachdev, and S. A. Kivelson, arXiv:1505.06206 [cond-mat.supr-con] (2015).

[154] G. Sordi, P. Sémon, K. Haule, and A.-M. S. Tremblay, Phys. Rev. B **87**, 041101 (2013).

[155] Y. Wang and A. Chubukov, Phys. Rev. B **90**, 035149 (2014).

[156] A. Allais, J. Bauer, and S. Sachdev, Phys. Rev. B **90**, 155114 (2014).

[157] V. S. de Carvalho and H. Freire, Nuclear Physics B **875**, 738 (2013).

[158] S. Whitsitt and S. Sachdev, Physical Review B **90**, 104505 (2014).

[159] V. S. de Carvalho, T. Kloss, X. Montiel, H. Freire, and C. Pépin, Phys. Rev. B **92**, 075123 (2015).

[160] P. A. Volkov and K. B. Efetov, arXiv:1511.01504 [cond-mat.str-el] (2015).

[161] P. W. Anderson, Physical Review **130**, 439 (1963).

[162] E. V. J. and K. S. A., Nature **374**, 434 (1995).

[163] Y. H. Liu, R. M. Konik, T. M. Rice, and F. C. Zhang, arXiv:1506.01258 [cond-mat.supr-con] (2015).

[164] M. R. Norman and C. Pépin, Rep. Prog. Phys. **66**, 1547 (2003).

[165] M. A. Metlitski and S. Sachdev, Phys. Rev. B **82**, 075128 (2010).

[166] J. S. e. a. Davis, preprint, to be published .

[167] X. Montiel, T. Kloss, and C. Pepin, preprint, to be published .

[168] Y. Tarutani et al., Appl. Phys. Lett. **58**, 2707 (1991).

[169] R. Yuasa et al., Physica C **185**, 2587 (1991).

[170] M. Kasai, Y. Kanke, T. Ohno, and Y. Kozono, J. Appl. Phys. **72**, 5344 (1992).

[171] A. Meltzow et al., Applied Superconductivity, IEEE Transactions on **7**, 2852 (1997).

[172] R. S. Decca, H. D. Drew, E. Osquiguil, B. Maiorov, and J. Guimpel, Phys. Rev. Lett. **85**, 3708 (2000).

[173] I. Bozovic et al., Phys. Rev. Lett. **93**, 157002 (2004).

[174] O. Tchernyshyov, M. R. Norman, and A. V. Chubukov, Phys. Rev. B **63**, 144507 (2001).

[175] Y. Wang, D. F. Agterberg, and A. Chubukov, Phys. Rev. B **91**, 115103 (2015).

[176] S. Kaiser et al., Phys. Rev. B **89**, 184516 (2014).

[177] R. D. Averitt et al., Phys. Rev. B **63**, 140502 (2001).

[178] A. Pashkin et al., Phys. Rev. Lett. **105**, 067001 (2010).

[179] C. M. Varma, P. B. Littlewood, S. Schmitt-Rink, E. Abrahams, and A. E. Ruckenstein, Phys. Rev. Lett. **63**, 1996 (1989).

[180] C. M. Varma, Phys. Rev. B **55**, 14554 (1997).

[181] H. Alloul, J. Bobroff, M. Gabay, and P. J. Hirschfeld, Rev. Mod. Phys. **81**, 45 (2009).

[182] C. Pépin and P. A. Lee, Phys. Rev. Lett. **81**, 2779 (1998).